Simultaneous characterization of optical and thermal parameters of liquid-crystal nanocolloids with high-temperature resolution

S. Paoloni, F. Mercuri, M. Marinelli, and U. Zammit
Dipartimento di Ingegneria Meccanica, Università di Roma "Tor Vergata," Roma, Italy

C. Neamtu and D. Dadarlat
National R&D Institute for Isotopic and Molecular Technologies, Cluj-Napoca, Romania
(Received 18 June 2008; published 23 October 2008)

We report on the high-temperature resolution measurements of the optical and thermal parameters of a liquid-crystal–silica nanoparticle colloid, as well as its video inspection, simultaneously performed in an upgraded photopyroelectric calorimeter. Over the nematic-isotropic coexistence region, the determined nematic correlation length, obtained from turbidity measurements, showed the characteristic two-step nematic nucleation process previously reported only for the specific heat.

DOI: 10.1103/PhysRevE.78.042701 PACS number(s): 64.70.M−, 61.30.Jf, 61.30.Pq

Investigations in nanostructured material, such as colloidal dispersions, often require the combination of different types of characterizations. Among them the measurements of thermal and optical properties seem particularly attractive especially in physical gels where they allow, for example, the study of the thermodynamics of the sol-gel transition and of the modification of the optical properties induced by the gel formation. Examples are the liquid-crystal (LC) gels obtained using low molecular mass organogelators [1] and nanocolloidal dispersions of particles in an anisotropic host [2], which have proved to be very interesting both as model systems and for applications.

When probing phase transitions of the host medium confined in a network, the optical and thermal parameters may show a strong temperature dependence in the vicinity of the transition temperature. High-temperature resolution measuring configurations are then required. Moreover, for a homogeneous comparison of the different characterizations, the experimental conditions in the different measuring systems, in terms of temperature resolution and also of sample composition, should be as similar as possible. For example, the nematic-isotropic (NI) transition in silica nanoparticles (aerosil) dispersed LC [2–4], where the LC molecules are aligned homeotropically at the particle surface, has attracted considerable interest because of the double-peak feature shown by the specific heat over the two-phase coexistence region. This indicated that the transition occurred in two steps: when cooling the sample, bulklike nematic material nucleates first over the high-temperature peak (HTP) while more strained nematic, lying close to the particle surfaces, nucleates over the low-temperature peak (LTP). In addition, high-temperature resolution polarization microscopy images [3], obtained simultaneously with calorimetric measurements performed in a photopyroelectric (PPE) setup [4], showed a nonmonotonic evolution of the nematic texture when cooling the sample from the isotropic phase, correlating well with the double-peak feature observed in the specific heat. The nematic domains were found to initially grow over the HTP region until they touched each other, and to break into smaller ones over the LTP region, the corresponding LC texture evolving from a coarse-grain to a fine-grain structure. This should imply a change in the nematic correlation length when crossing to the LTP region. However, no evidence of such change was detected in the nematic correlation length, ξ obtained by scattering measurements carried out on a sample that had showed the double-peak feature in the specific heat [5]. In fact, in a CCN47 (4'-transbutyl-4–cyano-4–heptylbicyclohexane) LC sample containing a particle concentration of 0.075 g/cm^3 (mass of particles/volume of LC), ξ revealed a monotonic change over the entire two-phase coexistence region until saturation occurred. The authors then concluded that the double-peaked feature on the specific heat was basically due to a change in the rate of the nucleation of nematic material with respect to temperature, in the two-phase coexistence region. This was associated to a crossover of the effect of disorder on the LC, from random dilution to random field regimes, with no change in the domain size.

In an effort to try and solve such an apparent discrepancy concerning the behavior of ξ over the LTP region, we present, in this Brief Report, the results of scattering measurements performed simultaneously with those of high-temperature resolution calorimetry of a LC nanocolloid sample performed in an upgraded photopyroelectric (PPE) set up. This enables highly temperature resolved characterizations of the optical as well as the thermal properties, and an accurate correlation of the different measured quantities at the various temperatures. The sample texture inspection was also carried out during the experiment.

Unlike standard ac calorimeters, the PPE technique enables the measurement of the specific heat, thermal conductivity, and thermal diffusivity, during a single run. Moreover, an improved data analysis procedure has been recently introduced [6] which allows also an indirect evaluation of latent heat and relaxation enthalpy, as well as the effective specific heat, involved over the phase transition. The basic idea of the new configuration of the PPE calorimeter is to exploit the optical access to the sample, necessary for the heating laser beam and already exploited for the imaging analysis, to insert a second beam which, passing through the sample, can probe its optical properties while the thermal characterization is carried out. This ensures identical experimental and

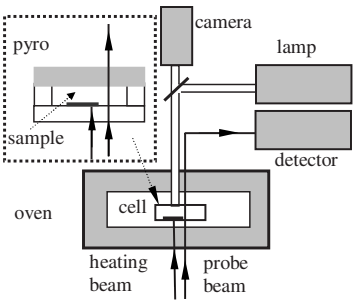

FIG. 1. Schematic view of the experimental setup.

sample conditions for the two characterizations. In phase transitions in LC, structure modifications, such as reorientation of anisotropic domains or the onset of two-phase coexistence, can generally affect the probe beam propagation. By detecting the transmitted beam, optical phenomena such as scattering or optical activity can be evaluated, thus enabling quantitative measurements associated to the sample morphology evolution [7]. Thanks to the characteristics of the new PPE setup, we present an accurate correlation of the double-step-like behavior in the specific heat and in the evolution of the sample texture grain size with the one we also detect in the nematic correlation length, unlike previous results.

Figure 1 shows the experimental setup. The sample, 8CB (4–octyl-4'-cyanobiphenyl) LC with an aerosil particle concentration of 0.02 g/cm^3, is contained in a 30-μm-thick, 1-cm-diameter quartz cell covered by a 300-μm-thick $LiTaO_3$ pyroelectric transducer. Only one-half of the cell surface in contact with the sample is coated with a Ti thin layer. The cell is illuminated by two distinct He-Ne laser beams, 3 mm apart, whose intensities are modulated at different frequencies in order to avoid any interference in the signals they give rise to. The first beam (heating beam) is absorbed by the Ti layer and periodically heats the sample surface in contact with the cell. The induced temperature oscillations, of the order of a few mK, are detected on the opposite sample surface by the pyroelectric transducer, allowing the straightforward determination of the thermal parameters according to the back-detection scheme model [8]. The second beam (probe beam) passes through the transparent side of the cell, the overlying sample, and the transducer coated with transparent indium-tin-oxide (ITO) electrodes to evaluate the optical turbidity. This basically relies on the beam intensity extinction due to the optical inhomogeneities scattering the light from the original beam path. In particular, after traveling over a distance d in the sample, the transmitted beam intensity is given by $I_T = I_0 \exp(-\tau d)$, where I_0 is the incident intensity and τ is the optical turbidity. The probe beam is first expanded and, after passing through the sample, is spatially filtered in order to retrieve the unaffected beam component. An optical detector, connected to a lock-in amplifier, detects the intensity transmitted through the aperture.

The cell is contained in an oven where the sample is heated at a rate typically of 1 mK/min. The sample is also continuously monitored during the temperature scan by the previously mentioned video imaging system [4], acting as a polarizing microscope operating in the reflection mode.

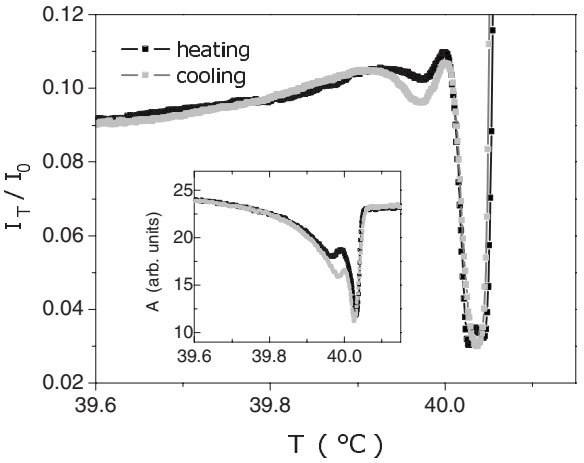

FIG. 2. Transmission (I_T/I_0) and PPE signal amplitude (A) (inset) vs temperature, simultaneously measured on an 8CB-aerosil mixture with a concentration of 0.02 g/cm^3. The heating and probe beams modulation frequencies were 31 Hz and 1.5 kHz, respectively.

Figure 2 shows the simultaneously detected probe beam transmission I_T/I_0 and PPE signal amplitude A (inset) obtained when heating and cooling the sample over the NI transition. The double-step feature, corresponding to the double peak in the specific heat, is evident in both the detected quantities together with the hysteretic behavior between heating and cooling runs of the sample, also observed in the measurements of the thermal parameters [3,9] and not reported in the scattering measurements presented in Ref. [5]. This indicates, in the present experimental conditions, a sufficient sensitivity of the scattering measurements to the different evolutions of the sample structure during the heating and cooling measurements. In the following, only the results relative to the cooling measurements will be discussed.

By processing the PPE signal amplitude and phase (not shown) data by means of a recently proposed procedure, the temperature-dependent profile, over the coexistence region, of the effective specific heat c_{eff} [6] and of the quantity I_L (which indirectly accounts for the latent heat or other kind of possible enthalpy exchange [6]) can be obtained, as shown in Fig. 3(a). In Fig. 3(b) the optical turbidity τ, obtained from the transmission data reported in Fig. 2, is shown together with the correspondingly calculated nematic correlation length ξ. A double steplike feature is clearly shown in the turbidity profile, similar to the one observed in the specific heat. Figures 4(a) and 4(b) present the polarization microscopy images obtained at the temperatures T_A and T_B indicated in Fig. 3. It is evident that, at temperature T_A, the expanding bulklike nematic domains have nearly saturated the available volume for free growth. We have limited the evaluation of ξ only in the temperature region below T_A where we could adopt a uniform profile for the nucleated nematic volume fraction Φ. In fact, in such a range, the residual latent-heat value is small and only minor changes in the $\Phi(T)$ profile should therefore be expected upon further cooling. For the evaluation of ξ, since the optical birefringence Δn of 8CB is about 10 times larger than that of

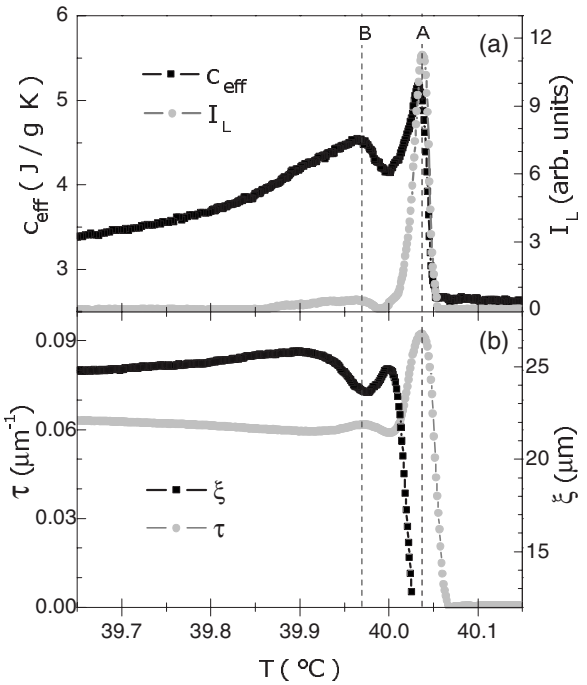

FIG. 3. Effective specific heat and internal source amplitude vs temperature (a) and optical turbidity and nematic correlation length (b), obtained from the data reported in Fig. 2, corresponding to the cooling run.

CCN47 LC used in Ref. [5], we have adopted the nonmonotonic relation between $\tau/\Delta n$ and $\xi\Delta n$ expressed by Eq. (47) in Ref. [10] corresponding to the composite model enabling us to correlate the above-mentioned quantities over the entire $\xi\Delta n$ range. According to such a relation, $\tau/\Delta n$ increases with $\xi\Delta n$ towards a maximum, beyond which the trend is inverted. In Ref. [10], Eq. (47) has been used for 6CB (4-hexyl-4'-cyanobiphenyl) which shows a birefringence value similar to that of 8CB. For our 8CB sample, as mentioned in Ref. [10], the presence of an inversion point in the turbidity for increasing ξ (decreasing temperature) over the peak value near T_{NI}, shown in Fig. 3(b), indicates that we are in the region where $\tau/\Delta n$ decreases with $\xi\Delta n$. Finally, similarly to the procedure adopted in Ref. [5], we have extrapolated the $\Delta n(T)$ profile obtained in the nematic range [11], also to the NI coexistence region where the value ranged around 0.11. The two-step process appearing in the thermal parameters and turbidity profiles, in the present case is also evident in the calculated profile of the correlation length shown in Fig. 3(b). Outside the coexistence region, the obtained saturation

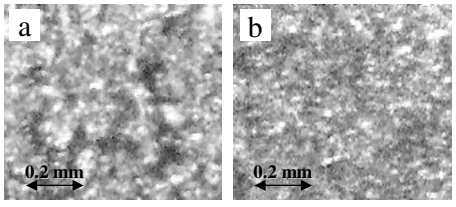

FIG. 4. Images of the sample's texture, obtained at the temperatures T_A (a) and T_B (b). The T_A and T_B values are identified in Figs. 3(a) and 3(b).

value, $\xi \approx 25$ μm in the nematic phase is very close to the one reported for 6CB LC with very similar concentration of aerosil particles [10]. We have also calculated $\xi(T)$ adopting a nonuniform $\Phi(T)$, obtained by integrating the latent-heat relative profile shown in Fig. 3(a), similarly to the procedure adopted in Ref. [5]. Though with different absolute values in the vicinity of T_A, $\xi(T)$ (not shown) qualitatively maintained a two-step-like profile, despite a variation in the rate of change of $\Phi(T)$ with temperature (not shown) observed over the LTP region, similar to that reported in Ref. [5]. We therefore believe that the $\Phi(T)$ behavior alone cannot account for the two-step-like profile observed in the specific heat, as suggested in Ref. [5], nor in that observed in the optical turbidity τ in the present work. It is important to point out that, though the reliability of the calculated absolute values of ξ, is affected by the appropriateness of the adopted model, the novelty of our results lies in the double-step-like profile obtained in the measured turbidity τ which has not been observed in the previous studies.

We have obtained the same two-step-like behaviors in ξ also for larger particle concentrations, with the saturation values in the nematic phases also approaching the corresponding ones reported in Ref. [10].

If the profiles of the various quantities reported in Fig. 3 are compared, the following scenario occurring over NI transition can be proposed. When cooling from the isotropic phase, the system enters the two-phase coexistence region where bulklike nematic domains nucleate and expand while their number rapidly increases. This gives rise to the fast increase of both I_L and τ, the latter reaching a maximum value at T_A when the expanding single domains tend to saturate the available volume for their free growth [Fig. 4(a)]. Correspondingly, c_{eff} is also found to grow rapidly with the steep part of its profile corresponding to the maximum of I_L where the release of latent heat is largest. Upon further cooling, the nucleated nematic domains start to coalesce thus leading to a local maximum of ξ, or equivalently to a local minimum of τ, due to the increased optical homogeneity of the sample. At lower temperature, also the LC close to the particle surface, which has a lower transition temperature because of its disorder, starts nucleating in strained nematic domains, as confirmed by the renewed increase of I_L and c_{eff}. These strained domains distort the existing ones to the extent that they break into smaller ones, relieving the strain and giving rise to the observed fine-grained texture [Fig. 4(b)]. Over such temperature range, I_L and c_{eff} approach their low-temperature peaks while ξ reaches the local minimum at T_B. At still lower temperatures the nematic correlation length tends towards the saturation value in the nematic phase, compatible with the given concentration of aerosil particles. It is also interesting to point out that the low-temperature peaks of I_L and c_{eff} are broader towards the lower-temperature region with respect to τ. In our opinion, as the temperature is lowered beyond the LTP, the average nematic domain size nucleating in the vicinity of the particle surface cannot substantially change, since it is strongly limited by the LC molecules pinning on the particle surface. The turbidity is therefore not significantly affected by the nucleation of the new nematic volumes, a process which, on the contrary, still significantly affects both c_{eff} and I_L.

A possible explanation for the detection of the double-step process also in the nematic correlation length found in this study, unlike the previously reported scattering results, could lie primarily in the fact that, owing to the considerably larger value Δn found in 8CB with respect to CCN47, a greater sensitivity of τ with respect to changes of ξ should be expected. The greater temperature resolution achieved in our PPE calorimetric setup and the fact that the optical and thermal parameters measurements were performed at the same time ensured a more accurate one-to-one correlation of the results concerning the different quantities obtained at each temperature.

In conclusion, thanks to an upgraded version of our PPE calorimeter, we have presented the simultaneous, high-temperature resolution characterization of the optical and thermal properties as well as the video inspection of a LC nanocolloid sample. This allowed us to correlate the two-step nematic nucleation process, previously observed in the specific heat over the NI coexistence region, to the one we have also observed in the nematic correlation length obtained by scattering measurements.

C.N. and D.D. acknowledge financial support by the Italian Ministry of Foreign Affairs, Directorate-General for Cultural Promotion and Cooperation, and Romanian National Authority for Scientific Research, Ministry of Education and Research, through Contract No. 12/2006 for mobility exchange under the 15th Italian-Romanian Executive Programme of S&T Cooperation.

[1] J. He, B. Yan, B. Yu, R. Bao, X. Wang, and Y. Wang, J. Colloid Interface Sci. **316**, 825 (2007).

[2] G. S. Iannacchione, C. W. Garland, J. T. Mang, and T. P. Rieker, Phys. Rev. E **58**, 5966 (1998), and references therein.

[3] F. Mercuri, S. Paoloni, U. Zammit, and M. Marinelli, Phys. Rev. Lett. **94**, 247801 (2005).

[4] F. Mercuri, R. Pizzoferrato, U. Zammit, and M. Marinelli, Appl. Phys. Lett. **81**, 4148 (2002).

[5] M. Caggioni, A. Roshi, S. Barjami, F. Mantegazza, G. S. Iannacchione, and T. Bellini, Phys. Rev. Lett. **93**, 127801 (2004).

[6] F. Mercuri, S. Paoloni, U. Zammit, F. Scudieri, and M. Marinelli, Phys. Rev. E **74**, 041707 (2006); F. Mercuri, M. Marinelli, S. Paoloni, U. Zammit, and F. Scudieri, Appl. Phys. Lett. **92**, 251911 (2008).

[7] T. Bellini and N. A. Clark, in *Liquid Crystals in Complex Geometries*, edited by G. P. Crawford and S. Zumer (Taylor & Francis, London, 1996), Chap. 19, and references therein.

[8] M. Marinelli, U. Zammit, F. Mercuri, and R. Pizzoferrato, J. Appl. Phys. **72**, 1096 (1992).

[9] M. Marinelli, F. Mercuri, S. Paoloni, and U. Zammit, Phys. Rev. Lett. **95**, 237801 (2005).

[10] T. Bellini, N. A. Clark, V. Degiorgio, F. Mantegazza, and G. Natale, Phys. Rev. E **57**, 2996 (1998).

[11] P. A. Karat and N. V. Madhusudana, Mol. Cryst. Liq. Cryst. **36**, 51 (1976).